

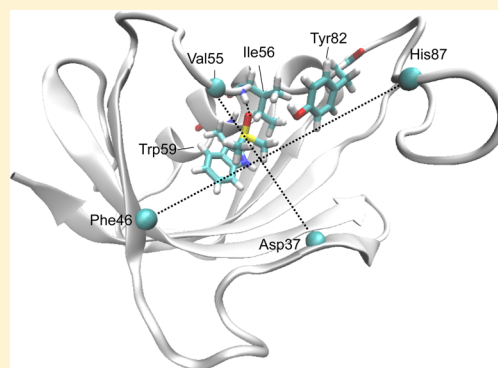
Protein Structural Memory Influences Ligand Binding Mode(s) and Unbinding Rates

Min Xu,[†] Amedeo Caflisch,^{*,†} and Peter Hamm^{*,‡}

[†]Department of Biochemistry and [‡]Department of Chemistry, University of Zürich, Winterthurerstrasse 190, Zürich CH-8057, Switzerland

Supporting Information

ABSTRACT: The binding of small molecules (e.g., natural ligands, metabolites, and drugs) to proteins governs most biochemical pathways and physiological processes. Here, we use molecular dynamics to investigate the unbinding of dimethyl sulfoxide (DMSO) from two distinct states of a small rotamase enzyme, the FK506-binding protein (FKBP). These states correspond to the FKBP protein relaxed with and without DMSO in the active site. Since the time scale of ligand unbinding (2–20 ns) is faster than protein relaxation (100 ns), a novel methodology is introduced to relax the protein without having to introduce an artificial constraint. The simulation results show that the unbinding time is an order of magnitude longer for dissociation from the DMSO-bound state (holo-relaxed). That is, the actual rate of unbinding depends on the state of the protein, with the protein having a long-lived memory. The rate thus depends on the concentration of the ligand as the apo and holo states reflect low and high concentrations of DMSO, respectively. Moreover, there are multiple binding modes in the apo-relaxed state, while a single binding mode dominates the holo-relaxed state in which DMSO acts as hydrogen bond acceptor from the backbone NH of Ile56, as in the crystal structure of the DMSO/FKBP complex. The solvent relaxes very fast (~1 ns) close to the NH of Ile56 and with the same time scale of the protein far away from the active site. These results have implications for high-throughput docking, which makes use of a rigid structure of the protein target.



1. INTRODUCTION

The association of endogenous ligands to enzymes and receptors regulates a large variety of biochemical pathways. Small-molecule drugs act by specific binding to a target protein to modulate their function, which is usually deregulated in the pathological state. Thus, the detailed analysis of ligand binding and the response of the target protein are expected to give insights useful for the understanding of biochemical processes (e.g., enzymatic reactions and signaling cascades) in the healthy and disease states.^{1–4}

Here, we analyze the kinetics and thermodynamics of DMSO unbinding from FKBP by explicit solvent molecular dynamics (MD) simulations. We have selected the 107-residue protein FKBP since there exists a high-resolution crystal structure of the complex with DMSO (PDB code 1D7H; Figure 1).⁵ FKBP is a peptidylprolyl isomerase (PPIase), whose name originates from the fact that it binds the immunosuppressant drug FK506 (also called tacrolimus). PPIases are present in many diverse organisms. There are two main classes of PPIases: FKBP^{6–8} and cyclophilins. These two classes are defined in terms of their artificial ligands, the natural products FK506 and cyclosporin A. These macrocyclic immunosuppressants inhibit the rotamase activity of their respective class but have no influence on the other class. Experimental evidence indicates that inhibition of the PPIase activity is not related to immunosuppression.⁹ On

the other hand, PPIases are important for accelerating the folding of some proteins^{10,11} for which the rate-limiting step involves the *trans* to *cis* isomerization of proline peptide bonds.^{10–12} Thus, FKBP is involved in protein folding and at the same time is an important small-molecule drug target.

In previous simulation studies, we have shown that unbinding of DMSO from FKBP required about 4 ns at 310 K, and multiple binding modes in the FKBP active site were observed.^{13,14} As an extension of that work, we present here multiple independent simulations of spontaneous DMSO unbinding starting from a protein ensemble that has been carefully equilibrated with either a DMSO molecule bound (i.e., in the holo-relaxed state) or in its apo-relaxed state. The simulations show that unbinding from the holo-relaxed state is an order of magnitude slower with the binding mode stabilized by a hydrogen bond with the backbone NH of Ile56. On the other hand, multiple binding modes are observed in the apo-relaxed state. We will furthermore show that upon unbinding from the holo-relaxed state the rearrangement of the FKBP binding site and water network are coupled, that is, both show similar relaxation kinetics. Moreover, the protein and water response is significantly slower than the DMSO unbinding

Received: November 5, 2015

Published: January 22, 2016

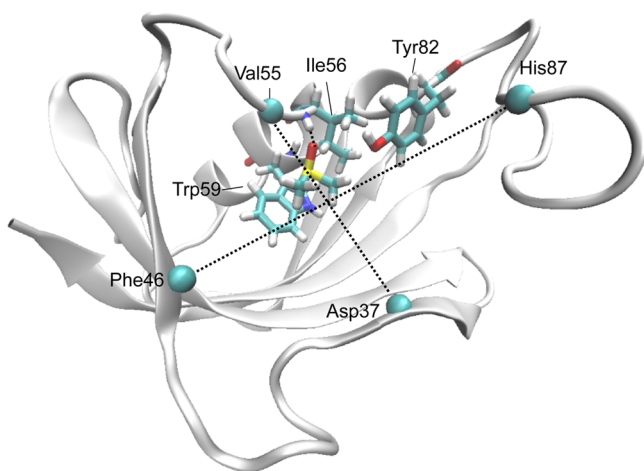


Figure 1. Crystal structure of the complex between FKBP and DMSO (PDB code 1D7H⁵). The DMSO molecule and side chains of Ile56, Trp59, and Tyr82 are shown in sticks. The hydrogen bond of DMSO to the backbone NH of Ile56 is shown by dotted lines. Also shown are the C_α atoms of Phe46, His87, Asp37, and Val55, the distances between which define the deformation of the binding groove after unbinding.

time. The results thus suggest that ligand unbinding is non-Markovian, and the term k_{off} becomes rather meaningless as the rate depends on the state of the protein, which in turn relaxes slower than unbinding itself.

2. METHODS

2.1. MD Setup. All the MD simulations involved in this study were performed using GROMACS 4.6.¹⁵ We used the CHARMM27 force field^{16,17} for the protein and CGENFF force field¹⁸ for the small molecule DMSO. The starting conformation was taken from the first chain of the X-ray crystal structure 1D7H (which has a DMSO molecule bound), and the water molecules close to the protein surface were kept. The system was solvated in a rhombic dodecahedron box with ≈ 7600 additional TIP3P water molecules¹⁹ together with 150 mM NaCl to neutralize the simulation box. We used 2 fs as the integration time step and the LINCS algorithm²⁰ to constrain the covalent bonds involving hydrogen atoms. Electrostatic interactions were approximated using the Particle-Mesh Ewald (PME) summation method,²¹ and van der Waals interactions were truncated with a cutoff of 10 Å. Before relaxation of the protein, the solvent was equilibrated for 1 ns with all the heavy atoms of the complex fixed around their position with a force constant of 1000 kJ/mol nm². All simulations were run as an NPT ensemble at a pressure of 1 atm using a Berendsen barostat with coupling time 2 ps and at a temperature of 273 K using velocity rescaling with a stochastic term²² with coupling time 0.1 ps. The low temperature is necessary to fully equilibrate the DMSO-bound state (see next subsection) because of previous unbinding simulations at 310 K, from which a k_{off}^{-1} of about 4 ns was determined.^{13,14} Note that the freezing point of TIP3P water is significantly lower than 273 K in the CHARMM27 force field.²³

2.2. Relaxation of Bound State. Starting from the solvent-equilibrated state, the goal was to relax the protein in its holo form (i.e., DMSO–protein complex) under the particular force field used in the simulation (which might result in a structure that deviates from the X-ray structure).

That was hampered by the fact that the average unbinding time of the unrelaxed protein was $k_{\text{off}}^{-1} = 15$ ns (Figure S1, Supporting Information), which turned out to be significantly too short to relax the protein. We therefore developed the following protocol: The simulation was run until the DMSO–protein distance exceeded some threshold. To that end, we used two distances, the distance r_{Trp59} of the S atom of the DMSO molecule to the center of the second ring of Trp59 as well as the hydrogen bond distance r_{Ile56} of the O atom of DMSO to the amide-proton of Ile56 (Figure 1), and we assumed unbinding when both distances exceeded 12 Å. Once unbinding occurred, we traced back the trajectory until both $r_{\text{Trp59}} < 3.5$ Å and $r_{\text{Ile56}} < 1.9$ Å. At that point of the trajectory, we reassigned new random velocities to all atoms of the simulation box according to a Boltzmann distribution at the same temperature $T = 273$ K (note that since kinetic and potential energy contributions to the partition function are separate reassigning new velocities and keeping the positions unchanged results in a canonical ensemble). With that initial condition, the MD simulation was launched again until the next unbinding event occurred, which is different and tentatively later than the previous one (Figure 2) since the new run produces a different trajectory. The procedure was continuously repeated.

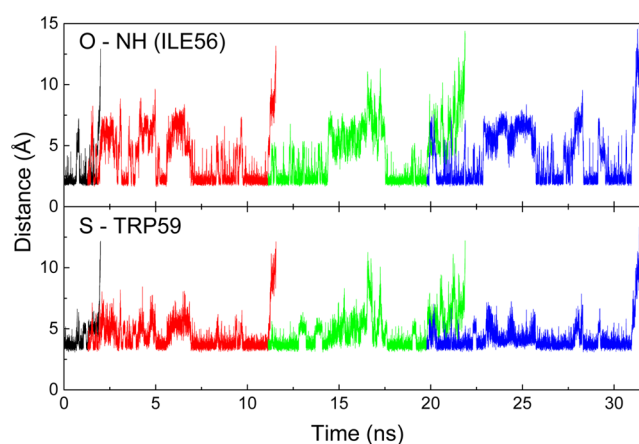


Figure 2. Example of four consecutive trajectories during the relaxation of the bound state, colored in black, red, green, and blue, showing the distances of the O atom of DMSO to the amide-proton of Ile56, r_{Ile56} (top), and that of the S atom of the DMSO molecule to the center of the 6-ring of Trp59, r_{Trp59} (bottom).

Following that protocol, we enable the protein to fully relax with DMSO bound to the protein all the time along that chain of simulations without having to invoke an artificial constraint to force the DMSO molecule to stay in the binding pocket. At the same time, the starting points of the individual simulation pieces serve as an ensemble of bound configurations used as starting points for the nonequilibrium simulations described in the next paragraph. In total, 116 such bound configurations have been collected from two independent chains of trajectories, each ≈ 1.4 μs long. Bound configurations from the first 200 ns were discarded to ensure that there is no bias from the initial X-ray structure.

2.3. Unbinding Simulations. Starting from the aforementioned 116 bound configurations, trajectories of 150 ns length have been simulated with 1 ps saving time and subsequently 500 ns with 10 ps saving time. By construct, this constitutes an ensemble of nonequilibrium trajectories

since all these 116 trajectories start from a bound state, while the equilibrium lies strongly on the unbound side. The k_{on} time for rebinding of the DMSO molecule is in the order of a few microseconds. Hence, out of the 116 trajectories, five such rebinding events occurred after the first 150 ns, and those trajectories have been discarded. For the remaining 111 trajectories, the DMSO has been removed and replaced by three water molecules after 150 ns to prevent rebinding within the subsequent 500 ns. The three water molecules replacing the DMSO molecule were placed at the positions of the oxygen atom and carbon atoms of the methyl groups. The three water molecules were then minimized and equilibrated by a MD run of 1 ns with the rest of the system frozen.

The final trajectories were synchronized by searching for the time point when both distances r_{Trp59} and r_{Ile56} first exceeded 20 Å (a looser criterion was used here to minimize events of immediate rebinding). From that time point, we traced back until both distances are still below 6 Å, which we defined as the time point of unbinding.

2.4. Rebinding Simulations. In order to also determine the unbinding constant for the apo-relaxed protein, the endpoint configurations of the 111 unbinding simulations described in the previous paragraph have been considered, all of which have been in the apo state for at least 500 ns, which is long enough to assume that the protein is indeed relaxed. A DMSO molecule has been reintroduced into these endpoint configurations replacing three water molecules, which form a triangle with their length all below 3.6 Å. Furthermore, in order to speed up the time for rebinding, only waters in the vicinity of the binding pocket were considered (i.e., with 13–21 Å from the C_{α} atoms of Asp37, Phe46, Val55, and His87). These three water molecules have been replaced by the oxygen and carbon atoms of the DMSO molecule with the RMSD minimized. Subsequently, the DMSO molecule as well as all water molecules and ions within 6 Å of the DMSO have been minimized and equilibrated for 1 ns, keeping all other atoms fixed. From that point, 30 ns long simulations were launched with random velocities assigned to all atoms. Typically $\approx 7\%$ of those simulations rebind during 30 ns, using a threshold of 6 Å for both r_{Trp59} and r_{Ile56} to determine binding. Trajectories that did not bind within 30 ns were relaunched with a new set of random velocities. That procedure was repeated seven times, collecting 58 rebinding events, whose subsequent unbinding was simulated as well. A table listing all simulations used for the study is given in Table S1 of the [Supporting Information](#).

2.5. Solvation Layer. In order to determine the water layer around the protein after unbinding from the holo-relaxed form, an average structure was first calculated from all snapshots before the time point of unbinding by aligning them upon each other, minimizing the RMSD of all C_{α} atoms. That average structure was considered to be the reference structure. Snapshot structures after the unbinding event were aligned to that reference structure and averaged in time bins on a logarithmic time axis (i.e., 10 bins per decade). Whenever aligning the protein backbone, the surrounding water molecules and the DMSO molecule were moved accordingly, and their densities have been calculated by binning them into cubes of 1 Å³. Figure S2 of the [Supporting Information](#) shows the RMSD of the structures within one time bin relative to the average in the same time bin, while the point at zero combines all structures before the unbinding event. The RMSD is quite small throughout (0.4 Å, which is consistent with the small B-factors in the 1D7H crystal structure,⁵ as 87% of the C_{α} atoms

have B-factor smaller than 30 Å²) and hardly changes during unbinding and during the relaxation of the protein; hence, the protein remains equally rigid at all times. This in turn evidences that the alignment procedure does not cause artifacts in the calculation of the water density around the protein.

3. RESULTS

3.1. Unbinding Constant and Binding Modes. Unbinding from the holo-relaxed state is about an order of magnitude slower ($k_{\text{off}}^{-1} = 23$ ns) than from the apo-relaxed state ($k_{\text{off}}^{-1} = 2.2$ ns) (Figure 3). Assuming that binding is diffusion-

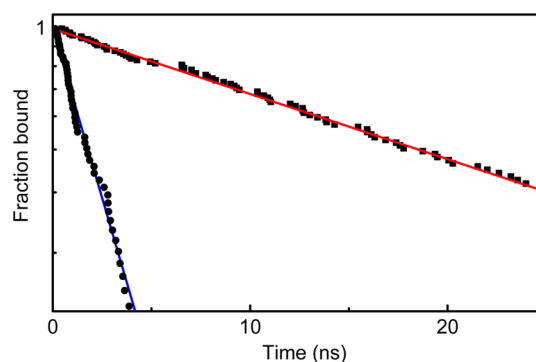


Figure 3. Fraction of bound DMSO molecules as a function of time, using a threshold of 12 Å for both r_{Trp59} and r_{Ile56} as a criterion of unbinding. The solid lines represent exponential fits with unbinding constants $k_{\text{off}}^{-1} = 23$ ns (red) for the holo-relaxed protein and $k_{\text{off}}^{-1} = 2.2$ ns (blue) for the apo-relaxed protein.

controlled and hence the same in both cases, the slow down by a factor 10 corresponds to a stabilization of the binding free energy in the holo-relaxed state by $\approx 2.3 k_{\text{B}}T \approx 1.3$ kcal/mol. This difference is significant given that the free energy of binding is only -0.8 kcal/mol as measured by nuclear magnetic resonance spectroscopy²⁴ or -2.3 kcal/mol measured by tryptophan fluorescence.⁵

Figure 4 shows projections of the free energy onto the two distances r_{Trp59} and r_{Ile56} evaluated along the trajectory segments during which the DMSO molecule is bound. Note that these free energy projections are not rigorously defined since the system is not in equilibrium during these time periods. These two-order parameters can resolve the various binding modes of the DMSO molecule reasonably well. That is, for the

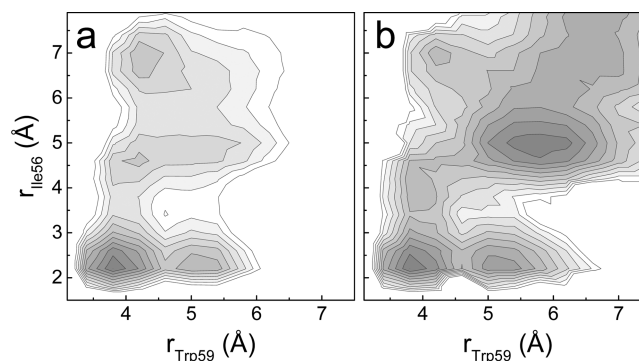


Figure 4. Histogram-based two-dimensional projection of the free energy along the two distances r_{Trp59} and r_{Ile56} for DMSO bound to the holo-relaxed protein (a) and apo-relaxed protein (b). Contour lines are separated by $0.5 k_{\text{B}}T$, starting from the corresponding minimum.

holo-relaxed protein (Figure 4a), the most populated binding mode (around $r_{\text{Trp59}} \approx 3.5$ Å and $r_{\text{Ile56}} \approx 2.2$ Å) corresponds to the crystal structure (PDB code 1D7H) in which the oxygen atom of DMSO is involved as acceptor in a hydrogen bond with the NH group of Ile56 (Figure 1). The free energy surface is quite different in the apo-relaxed form (Figure 4b). The minimum with hydrogen bond to the NH of Ile56 still exists but is less populated as only 3 out of 58 trajectories visited that minimum (Methods section). Importantly, a new metastable state is populated ($r_{\text{Trp59}} \approx 5.8$ Å and $r_{\text{Ile56}} \approx 5.0$ Å) in which the oxygen atom of DMSO accepts a hydrogen bond from the hydroxyl group of Tyr82 (see Figure 1 as well as Figure S3, Supporting Information). This state is essentially absent for the holo-relaxed protein. The free-energy difference from the minimum with hydrogen bond to Tyr82 to a fully dissociated state is only $\approx 1.5 k_B T$, along the “channel” guiding toward the top-right corner of Figure 4b, which explains at least in part the faster unbinding from the apo-relaxed state.

3.2. Slow Response of the Protein. The actual event of unbinding takes roughly a nanosecond (Figure 2). Subsequently, the binding groove relaxes by becoming a bit larger in the one direction (Phe46–His87), and a bit smaller in a perpendicular direction (Asp37–Val55) (Figure 5a). The

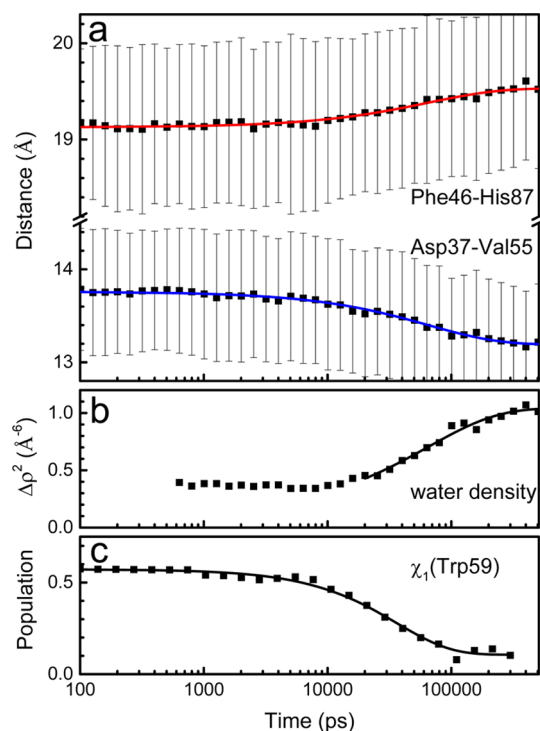


Figure 5. Protein and water relaxation upon DMSO unbinding from the holo-relaxed state. (a) Time dependence of the average C_α – C_α distance between two pairs of amino acids (Phe46–His87 and Asp37–Val55) across the binding groove. The bars indicate the $\pm \sigma$ -interval of the fluctuations around the average. (b) Squared water density change $\Delta\rho^2$ integrated around the protein. In panels (a) and (b), the solid lines show a global stretched-exponential fit to the data, revealing a time constant of $\tau = 65$ ns and a stretching factor $\beta = 0.77$. The data <20 ns in panel (b) were discarded, as the initial small drop in $\Delta\rho^2$ is an artifact from the decreasing background noise due to the better averaging in the exponentially increasing time bins. (c) Time dependence of the population of the gauche⁻ conformer of the Trp59 χ_1 dihedral angle. The solid line is a single-exponential fit with time constant of 36 ns.

structural changes are small, that is, $\lesssim 1$ Å, but clearly resolvable. The relaxation process takes a few 100 ns to finish and proceeds in a nonexponential manner. Globally fitting the two distance traces with a stretched-exponential function $S(t) = A \exp(-(t/\tau)^\beta) + A_0$ reveals a time constant of $\tau = 65$ ns and a stretching factor of $\beta = 0.77$ that deviates significantly from 1. With these values, we obtain for the mean relaxation time $\langle \tau \rangle \equiv \int_0^\infty t e^{-(t/\tau)^\beta} dt = \tau/\beta \Gamma(1/\beta) = 75$ ns.²⁵ Importantly, the mean relaxation time is significantly slower than the unbinding constant $k_{\text{off}}^{-1} = 23$ ns.

The side chain of Trp59, which forms the “floor” of the DMSO (and substrate) binding site (Figure 1), changes its orientation upon DMSO unbinding with a time scale that is slower than the dissociation but slightly faster than the relaxation of the binding site. The reorientation of the Trp59 side chain, namely, the changes of χ_1 from gauche⁻ to trans and χ_2 from about 40° to 0° (Figure S4), is completed in about 100 ns and can be fitted by a single-exponential function with a time constant of 36 ns (Figure 5c). The single-exponential fitting is consistent with a single free energy barrier between the two rotameric states of the Trp59 side chains.

3.3. Solvent Relaxation Coupled to the Protein Response. The temporal evolution of the radial distribution function of the water molecules around the NH of Ile56 (Figure S5a) shows that the rearrangement of the first solvation layer around the Ile56 amide, that is, binding of two to three water molecules, occurs almost simultaneously with the unbinding of DMSO, and is nearly 2 orders of magnitude faster than the full relaxation of the protein. In striking contrast, the relaxation of the solvation layer far away from the DMSO binding site is slow and keeps evolving on a few 100 ns time scale (Figure S6). At about 50 ns, the water density has started to change almost everywhere around the protein, as exemplified for Gly62 and Tyr26 both of which are situated on the protein surface opposite from the binding pocket (Figure S5bc). The change of water density integrated over the whole protein surface shows that this change proceeds essentially simultaneously as the protein undergoes its conformational transition. As a matter of fact, it can be fitted with the same stretched-exponential function with time constant of $\tau = 65$ ns and stretching factor of $\beta = 0.77$ (Figure 5b).

To further investigate the relationship between protein and solvent responses, an additional set of unbinding simulations was carried out with restraints on the protein backbone. In the active site, water still exchanges with DMSO, leading to qualitatively similar results for the water density as in the unrestrained simulations, but essentially nothing happens later on around the protein (Figure S7). These control simulations provide additional evidence that the change in the protein solvation shell and the protein conformation itself are inherently coupled to each other.

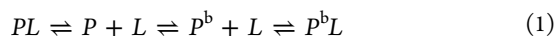
4. DISCUSSION AND CONCLUSION

We have carried out multiple MD simulations of DMSO unbinding from two distinct conformations of FKBP, namely, the apo state and DMSO-bound or holo-relaxed state. The MD trajectories were used to extract the unbinding kinetics and analyze the response of the protein and change of the solvent density around it. Four main observations emerge from our simulation study:

- (1) Despite the fact that the structural changes of the binding pocket are relatively small ($\lesssim 1$ Å), they have a significant

effect on the DMSO unbinding constant (Figure 3). The differences in the binding site influence the relative weights of the binding modes of DMSO, which are different in the holo-relaxed and apo-relaxed states (Figure 4). The binding mode in the holo-relaxed state is dominated by the direct hydrogen bond to the NH group of Ile56, which is consistent with the X-ray structure (PDB code 1D7H) and previous atomistic simulations carried out at a DMSO concentration of 0.44 M.¹⁴ In the apo-relaxed state, there is a highly populated binding mode in which the DMSO molecule acts as hydrogen bond acceptor for the side chain hydroxyl of Tyr82. This binding mode is kinetically less stable than the one with the hydrogen bond to the NH group of Ile56 (Figure 4).

It is interesting to analyze the mechanism of DMSO (L) binding to FKBP (P), which on the basis of the simulation results can be described by



where P and P^b represent the apo and ligand-bound state, respectively. Because the unbinding time from the apo state (2.2 ns) and from the holo state (23 ns) are faster than the relaxation of the protein (middle double arrow, 75 ns), the saturation (Y) of the protein has a hyperbolic dependence on the ligand concentration $[L]$, that is, $Y = [L]/(K_D + [L])$, both at low and high concentrations of the ligand but with different values of the dissociation constant (K_D). In other words, the equilibrium is shifted almost completely to the left or right of eq 1 at low or high concentration of DMSO, respectively. Crucially, at intermediate concentrations of the ligand, for example, during a rapid switch in concentration, memory effects will influence the ligand saturation. On the other hand, FKBP is not an hysteretic enzyme in its original definition²⁶ because the time scale of relaxation upon ligand (DMSO) unbinding (75 ns) is much faster than the reciprocal of the turnover number of the peptidylprolyl isomerase reaction, which is about 10 ms.²⁷

- (2) The binding/unbinding of DMSO, a small molecule of only four non-hydrogen atoms, has a sizable effect on the protein structure. This observation has important consequences for automatic docking, which is usually performed with a single rigid structure of the protein receptor. In the literature, there are a few examples of high-throughput docking campaigns that made use of multiple protein structures originating from MD simulations and differing from the crystal structure (see ref 28 for a recent review). Crucially, the small-molecule inhibitors identified in those docking campaigns do not fit sterically into the binding site of the original crystal structure.^{29–31} In other words, the active compounds discovered in our previous studies, in which the binding site was previously relaxed by MD, would have been false negatives if the docking would have used the rigid crystal structure. Here, we have introduced an MD simulation protocol to “prepare” a protein for docking by relaxation of its complex with a small molecule. The protocol, which consists of the iterative restarting of MD simulations of unbinding, generates a fully relaxed bound state. For the docking of a library of fragments that are similar to the small molecule employed in the

equilibration procedure, the use of the equilibrated bound state is more appropriate and will result in less false negatives than the use of the crystal structure of the apo protein. For ligands that have slow unbinding times ($\geq 1 \mu\text{s}$), it is probably sufficient to equilibrate the bound state in a single run starting from the crystal structure of the complex.

- (3) With a mean relaxation time of $\langle\tau\rangle = 75$ ns, the rearrangement of the protein and its solvation layer is nearly 2 orders of magnitude slower than the actual process of unbinding (≈ 1 ns) and also significantly slower than the dissociation time $k_{\text{off}}^{-1} = 23$ ns. This renders the process non-Markovian, and terms like k_{on} and k_{off} become essentially meaningless, as the actual rate depends on the conformational state of the protein (to which it relaxes with the ligand either bound or unbound), which in turn has a long-lived memory. Importantly, the unbinding time becomes a function of the ligand concentration; it is significantly longer at high concentration of DMSO (holo-relaxed) than at low concentration (apo-relaxed).
- (4) The first layer of water molecules and atoms on the protein surface relax concomitantly. Thus, the first solvation layer has to be viewed as an integral part of the protein.³² In other words, the relaxation of the protein surface is not governed by solvent (or vice versa). The relaxation is rather a coupled rearrangement of hydrogen bonds of water molecules and polar groups of the protein (intraprotein and protein–water). The question of the size and properties of the solvation layer has been investigated extensively and discussed in a rather controversial manner over the past years using, for example, NMR spectroscopy,³² THz spectroscopy,³³ and MD simulations.^{34–36} In particular, our results are congruent with the concept of the “slaving” of water and protein motions originally introduced by Frauenfelder, Wolynes, and co-workers.^{37,38}

Overall speaking, the response we see here for unbinding of DMSO from FKBP is precisely the same as that for a photoswitchable PDZ2 domain that we have studied recently.^{39,40} In that PDZ2 domain, an azobenzene derivative has been covalently linked across its binding groove in a way to mimic a structural change that roughly equals that upon ligand binding/unbinding of the native system. While that molecular construct has been artificial, it has the feature that it can be triggered by light on a picosecond time scale and as such allowed us to study the time response experimentally by transient IR spectroscopy. In ref 39, we obtained a semi-quantitative agreement between the experiments and accompanying MD simulations, which in turn compare well with the MD simulation of the present study for FKBP. That is, we observe the same 100 ns time scale for the response of the binding pocket in both cases, relaxation proceeds in a nonexponential manner, and the size of the structural change is also very comparable with about 1 Å. Also the response of the first solvation layer (Figure S6) is qualitatively the same. This agreement evidences that on the one hand the molecular construct of ref 39 mimics the dynamics of ligand binding reasonably well and on the other hand suggests that the 100 ns time scale is rather general, at least for single-domain proteins of about 100 residues.

It is interesting to relate these results to commonly discussed mechanisms of ligand binding, that is, “induced fit” versus “conformational selection”.⁴¹ According to Onsager’s regression hypothesis, the relaxation of a nonequilibrium ensemble toward equilibrium equals the equilibrium correlation function, $\langle x(t) \rangle_{\text{nonequ}} \propto \langle x(0)x(t) \rangle_{\text{equ}}$.⁴² To that end, it is important to note that the holo-relaxed state effectively constitutes a nonequilibrium ensemble (at low concentration of DMSO), which relaxes toward equilibrium after unbinding of the DMSO molecule. But the size of the structural change on average is of the same order of magnitude as the fluctuations once equilibrium is reached (see bars in Figure 5a); hence, linear response theory applies. We thus can assume that the relaxation kinetics of the opposite process, that is, upon ligand binding, would be the same as that upon ligand unbinding, which we investigated here (just that the DMSO molecule would not stay long enough for full relaxation to occur; Figure 3, blue). In that sense, what we observe here is an “induced fit” mechanism.⁴¹ That is, the protein adapts to a binding event only relatively slowly by lowering the binding free energy and thereby stabilizing the bound state. The question whether it is an induced fit mechanism, however, depends on time scales and concentration of the ligand. DMSO has a very small binding affinity. Hence, its residence time at the protein is short, and the slow relaxation of the protein does indeed matter. On the other hand, for a ligand with much higher binding affinity, the residence time will be significantly longer. Once it exceeds the relaxation time of the protein, the process is effectively Markovian. As the structural change upon ligand binding is smaller than the equilibrium fluctuations, the holo-structure of the protein will occasionally appear even in the apo-relaxed form. The mechanism of ligand binding then turns into “conformational selection”.⁴¹

■ ASSOCIATED CONTENT

Supporting Information

The Supporting Information is available free of charge on the ACS Publications website at DOI: 10.1021/acs.jctc.5b01052.

Table listing all the simulations performed in this study and figures of the detailed analysis results. (PDF)

■ AUTHOR INFORMATION

Corresponding Authors

*Phone: (+41 44) 635 55 68. Fax: (+41 44) 635 68 62. E-mail: caflisch@bioc.uzh.ch (A.C.).

*Phone: (+41 44) 635 55 68. Fax: (+41 44) 635 68 62. E-mail: peter.hamm@chem.uzh.ch (P.H.).

Notes

The authors declare no competing financial interest.

■ ACKNOWLEDGMENTS

The work has been supported by an ERC advanced investigator grant (DYNALLO) and by the Swiss National Science Foundation through the NCCR MUST to P.H., as well as by the Swiss National Science Foundation to A.C. We are grateful for insightful discussions with Andreas Vitalis, Steven Waldauer, and Brigitte Stucki-Buchli.

■ REFERENCES

- (1) Fersht, A. *Structure and Mechanism in Protein Science*; W. H. Freeman and Company: New York, 1999.
- (2) Henzler-Wildman, K.; Kern, D. Dynamic personalities of proteins. *Nature* **2007**, *450*, 964–972.
- (3) Seo, M.-H.; Park, J.; Kim, E.; Hohng, S.; Kim, H.-S. Protein conformational dynamics dictate the binding affinity for a ligand. *Nat. Commun.* **2014**, DOI: 10.1038/ncomms4724.
- (4) Plattner, N.; Noe, F. Protein conformational plasticity and complex ligand-binding kinetics explored by atomistic simulations and Markov models. *Nat. Commun.* **2015**, *6*, 7653.
- (5) Burkhard, P.; Taylor, P.; Walkinshaw, M. D. X-ray structures of small ligand-FKBP complexes provide an estimate for hydrophobic interaction energies. *J. Mol. Biol.* **2000**, *295*, 953–62.
- (6) Siekierka, J. J.; Hung, S. H. Y.; Poe, M.; Lin, C. S.; Sigal, N. H. A cytosolic binding protein for the immunosuppressant FK506 has peptidyl-prolyl isomerase activity but is distinct from cyclophilin. *Nature* **1989**, *341*, 755–757.
- (7) Harding, M. W.; Galat, A.; Uehling, D. E.; Schreiber, S. L. A receptor for the immuno-suppressant FK506 is a cis-trans peptidyl-prolyl isomerase. *Nature* **1989**, *341*, 758–760.
- (8) Clardy, J. The chemistry of signal transduction. *Proc. Natl. Acad. Sci. U. S. A.* **1995**, *92*, 56–61.
- (9) Schreiber, S. L.; Crabtree, G. R. The mechanism of action of cyclosporin A and FK506. *Immunol. Today* **1992**, *13*, 136–142.
- (10) Fischer, G.; Wittmann-Liebold, B.; Lang, K.; Kiefhaber, T.; Schmid, F. X. Cyclophilin and peptidyl-prolyl cis-trans isomerase are probably identical proteins. *Nature* **1989**, *337*, 476–478.
- (11) Tropschug, M.; Wachter, E.; Mayer, S.; Schonbrunner, E. R.; Schmid, F. X. Isolation and sequence of an FK506-binding protein from *N. crassa* which catalyses protein folding. *Nature* **1990**, *346*, 674–677.
- (12) Lang, K.; Schmid, F. X.; Fischer, G. Catalysis of protein folding by prolyl isomerase. *Nature* **1987**, *329*, 268–270.
- (13) Huang, D.; Caflisch, A. The free energy landscape of small molecule unbinding. *PLoS Comput. Biol.* **2011**, *7*, e1002002.
- (14) Huang, D.; Caflisch, A. Small molecule binding to proteins: Affinity and binding/unbinding dynamics from atomistic simulations. *ChemMedChem* **2011**, *6*, 1578–1580.
- (15) Van Der Spoel, D.; Lindahl, E.; Hess, B.; Groenhof, G.; Mark, A. E.; Berendsen, H. J. C. GROMACS: Fast, flexible, and free. *J. Comput. Chem.* **2005**, *26*, 1701–1718.
- (16) MacKerell, A. D.; Feig, M.; Brooks, C. L., III Extending the treatment of backbone energetics in protein force fields: Limitations of gas-phase quantum mechanics in reproducing protein conformational distributions in molecular dynamics simulations. *J. Comput. Chem.* **2004**, *25*, 1400–1415.
- (17) Mackerell, A. D.; Bashford, D.; Bellott, M.; Dunbrack, R. L.; Evanseck, J. D.; Field, M. J.; Fischer, S.; Gao, J.; Guo, H.; Ha, S.; Joseph-McCarthy, D.; Kuchnir, L.; Kuczera, K.; Lau, F. T. K.; Mattos, C.; Michnick, S.; Ngo, T.; Nguyen, D. T.; Prodhom, B.; Reiher, W. E.; Roux, B.; Schlenkrich, M.; Smith, J. C.; Stote, R.; Straub, J.; Watanabe, M.; Wiórkiewicz-Kuczera, J.; Yin, D.; Karplus, M. All-atom empirical potential for molecular modeling and dynamics studies of proteins. *J. Phys. Chem. B* **1998**, *102*, 3586–3616.
- (18) Vanommeslaeghe, K.; Raman, E. P.; MacKerell, A. D. Automation of the CHARMM General Force Field (CGenFF) II: Assignment of bonded parameters and partial atomic charges. *J. Chem. Inf. Model.* **2012**, *52*, 3155–3168.
- (19) Jorgensen, W. L.; Chandrasekhar, J.; Madura, J. D.; Impey, R. W.; Klein, M. L. Comparison of simple potential functions for simulating liquid water. *J. Chem. Phys.* **1983**, *79*, 926–935.
- (20) Hess, B.; Bekker, H.; Berendsen, H. J. C.; Fraaije, J. G. E. M. LINCS: A linear constraint solver for molecular simulations. *J. Comput. Chem.* **1997**, *18*, 1463–1472.
- (21) Darden, T.; York, D.; Pedersen, L. Particle mesh Ewald: An Nlog(N) method for Ewald sums in large systems. *J. Chem. Phys.* **1993**, *98*, 10089–10092.
- (22) Bussi, G.; Donadio, D.; Parrinello, M. Canonical sampling through velocity rescaling. *J. Chem. Phys.* **2007**, *126*, 014101.
- (23) Vega, C.; Sanz, E.; Abascal, J. L. F. The melting temperature of the most common models of water. *J. Chem. Phys.* **2005**, *122*, 114507.

(24) Dalvit, C.; Floersheim, P.; Zurini, M.; Widmer, A. Use of organic solvents and small molecules for locating binding sites on proteins in solutions. *J. Biomol. NMR* **1999**, *14*, 23–32.

(25) Alvarez, F.; Alegria, A.; Colmenero, J. Relationship between the time-domain Kohlrausch-Williams-Watts and frequency-domain Havriliak-Negami relaxation functions. *Phys. Rev. B: Condens. Matter Mater. Phys.* **1991**, *44*, 7306–7312.

(26) Frieden, C. Kinetic aspects of regulation of metabolic processes: The hysteretic enzyme concept. *J. Biol. Chem.* **1970**, *245*, 5788–5799.

(27) Petros, A. M.; Luly, J. R.; Liang, H.; Fesik, S. W. Conformation of an FK506 analog in aqueous solution is similar to the FKBP-bound conformation of FK506. *J. Am. Chem. Soc.* **1993**, *115*, 9920–9924.

(28) Zhao, H.; Cafilisch, A. Molecular dynamics in drug design. *Eur. J. Med. Chem.* **2015**, *91*, 4–14.

(29) Ekonomiuk, D.; Su, X.-C.; Ozawa, K.; Bodenreider, C.; Lim, S. P.; Otting, G.; Huang, D.; Cafilisch, A. Flaviviral protease inhibitors identified by fragment-based library docking into a structure generated by molecular dynamics. *J. Med. Chem.* **2009**, *52*, 4860–4868.

(30) Zhao, H.; Cafilisch, A. Discovery of ZAP70 inhibitors by high-throughput docking into a conformation of its kinase domain generated by molecular dynamics. *Bioorg. Med. Chem. Lett.* **2013**, *23*, 5721–5726.

(31) Zhao, H.; Cafilisch, A. Discovery of dual ZAP70 and Syk kinases inhibitors by docking into a rare C-helix-out conformation of Syk. *Bioorg. Med. Chem. Lett.* **2014**, *24*, 1523–1527.

(32) Halle, B. Protein hydration dynamics in solution: a critical survey. *Philos. Trans. R. Soc., B* **2004**, *359*, 1207–1224.

(33) Ebbinghaus, S.; Kim, S. J.; Heyden, M.; Yu, X.; Heugen, U.; Gruebele, M.; Leitner, D. M.; Havenith, M. An extended dynamical hydration shell around proteins. *Proc. Natl. Acad. Sci. U. S. A.* **2007**, *104*, 20749–20752.

(34) Brooks, C. L., III; Karplus, M. Solvent effects on protein motion and protein effects on solvent motion. *J. Mol. Biol.* **1989**, *208*, 159–181.

(35) Vitkup, D.; Ringe, D.; Petsko, G. A.; Karplus, M. Solvent mobility and the protein ‘glass’ transition. *Nat. Struct. Biol.* **2000**, *7*, 34–38.

(36) Heyden, M. Resolving anisotropic distributions of correlated vibrations in protein hydration water. *J. Chem. Phys.* **2014**, *141*, 22D509.

(37) Fenimore, P. W.; Frauenfelder, H.; McMahon, B. H.; Parak, F. G. Slaving: Solvent fluctuations dominate protein dynamics and functions. *Proc. Natl. Acad. Sci. U. S. A.* **2002**, *99*, 16047–16051.

(38) Lubchenko, V.; Wolynes, P. G.; Frauenfelder, H. The mosaic energy landscapes of liquids and the control of protein conformational dynamics by glass forming solvents. *J. Phys. Chem. B* **2005**, *109*, 7488–7499.

(39) Buchli, B.; Waldauer, S. A.; Walser, R.; Donten, M. L.; Pfister, R.; Blöchliger, N.; Steiner, S.; Cafilisch, A.; Zerbe, O.; Hamm, P. Kinetic response of a photoperturbed allosteric protein. *Proc. Natl. Acad. Sci. U. S. A.* **2013**, *110*, 11725–11730.

(40) Waldauer, S. A.; Stucki-Buchli, B.; Frey, L.; Hamm, P. Effect of viscogens on the kinetic response of a photoperturbed allosteric protein. *J. Chem. Phys.* **2014**, *141*, 22D514.

(41) Csermely, P.; Palotai, R.; Nussinov, R. Induced fit, conformational selection and independent dynamic segments: An extended view of binding events. *Trends Biochem. Sci.* **2010**, *35*, 539–546.

(42) Chandler, D. *Introduction to Modern Statistical Mechanics*; Oxford University Press: Oxford, 1987.